VALORIZATION OF CARBON DIOXIDE THROUGH ELECTROCATALYTIC CONVERSION: COPPER ELECTROCATALYSTS SUPPORTED IN GRAPHENE

Viviana Alejandra Méndez Torres[1]; Franz Edwin López Suarez[2]

[1]Department of Engineering, Chemical engineering Program, Universidad Jorge Tadeo Lozano, Bogota - Colombia

Abstract

Carbon dioxide is one of the main causes of global warming. An alternative to decrease your concentration is by means electro-reduce technology, which produce organic compounds with higher energy density. In this process, the use of electrocatalysts is required, where its composition and structure are fundamental for good performance, efficiency and productivity. The use of carbonaceous materials provides the best support for this type of applications due to its specific properties. It object of this work to carry out the synthesis and characterization of copper electrocatalysts (10% m/v) supported on graphene. The graphene is synthesized from graphite (electrochemical and commercial source). Electrocatalysts using other carbonaceous materials such as carbon nanotubes and carbon blacks have been prepared for purpose of comparison. The materials have been characterized by X-ray diffraction (XRD), Raman spectroscopy, infrared spectroscopy (FTIR) and scanning electron microscopy (SEM).

Keywords: Electro-conversion of CO_2, graphene, nanotubes, electrocatalysts.

1. Introduction

The conversion of carbon dioxide into the value of the product has been of great interest in recent years because the annual emissions of this greenhouse gas generate a negative impact on the environment. Due to this problem, different solutions have been proposed, among them, the biological conversion, the chemical conversion and the catalytic conversion. Being the most attractive of all the conversions, electrocatalytic conversion, which consists in fixing the carbon dioxide in an electrochemical cell, where the gas reduction occurs in the cathode with H^+ and the energy coming from the oxidation of water in the anode producing organic compounds with higher energy density [1].

In this process, catalysts are required to improve the process of electroreduction of carbon dioxide. The use of carbonaceous materials such as graphite, carbon nanotubes and activated carbon to support active phase have shown high reliability [2] due to their specific properties, such as porosity, the conductivity and others [3] guaranteeing optimal performance. Especially graphene, which is a sheet of carbon with a thickness of a single atom, which facilitates the improvement of properties [4]. The combination of carbonaceous supporting metals provides the electrocatalyst with stability and activity in electroconversion. Different metals have been used as phase active, such as platinum, cobalt, iron and copper [5]. It is important to focus the use of different metals in the electrocatalysts due to the interactions of the metal with the carbon support improve the rearrangement of the structure,

decreases the surface energy and presents an increase in the electrocatalytic activity of the material used [6].

The objective of this work was the synthesis and characterization of electrocatalysts varying the carbon support between commercial and electrochemical graphene, carbon nanotubes and activated carbon. Electrocatalysts were synthesized using copper nitrate in a 10% m/v solution as metal precursor. These materials were characterized to determine the crystallinity structure by X-ray diffraction and Raman spectroscopy, functional groups by infrared spectroscopy (FTIR) and finally a high-resolution image of the surface of the samples by scanning electron microscopy (SEM).

2. Experimental

2.1 Preparation of graphene oxide

Graphene oxide was produced using the modified Hummer method [7]. 0.5 g of graphite was dissolved in 20 mL of sulfuric acid (96% H_2SO_4) for 24 hours under constant agitation, then 2.5 g of potassium permanganate ($KMNO_4$ 99%) were added maintaining the agitation without exceeding the temperature of 35°C (controlled with ice bath). After heating for an hour at a temperature of 65°C approximately, 2.5 ml of hydrogen peroxide (H2O2 30% v / v) are added, stirring slowly until the yellow bubbling stops. The sample was centrifuged, discarding the supernatant and leaving the precipitate. The sample was washed with a hydrochloric acid (5% w/w HCl), the solid was dried at 100°C for 24 hours. The graphite used as precursor are a commercial and electrochemical. The commercial graphite purchased from a local store and the electrochemical graphite obtained from graphite electrodes that comes from the petroleum industry as a by-product from the oil refining process.

2.2 Preparation of reduced graphene

The synthesis of the reduced graphene was carried out according to the following procedure. 100 mg of graphene oxide are dissolved in 50 mL of distilled water in order to obtain a concentration of 2mg/mL. This solution was placed in ultrasound for 1 hour and centrifuged at a speed of 1000 rpm for 5 minutes discarded the supernatant phase. In order to adjust the pH of the solution to 10, ammonium hydroxide (30% v/v) is added. Subsequently, sodium borohydride was added (reducing agent) and the solution is placed in an autoclave at 100°C for 3 hours. The sample was consecutively centrifuged for 5 minutes at a speed of 2500 rpm, separated and washed with distilled water from 4 to 5 times. Finally, the samples obtained was dried for 24 hours at 40°C [8]. The nomenclature used to identify the samples is: V1GO and V6 GO, (samples corresponds to the commercial graphene oxide) and V3 EGO and V8 EGO (samples electrochemical graphene oxide).

2.3 Preparation of carbon nanotubes

The method used for the synthesis of carbon nanotubes was realized by catalytic decomposition of acetylene, which is the source of carbon. It was carried out by means of a reactor inside a furnace, there nitrogen was mixed at a flow rate of 3850 cm^3/min and hydrogen at a flow rate of 40 cm^3/min, and this being the carrier gas while iron catalyst precursor was used iron pentacarbonyl. The metal catalyst was introduced through the liquid carbonyl in the reaction zone at a temperature of 0°C [9]. In the reactor, the cordierite

monoliths were placed in the open channels in the same direction of the gas flow while the metal catalyst precursors were thermally decomposed in order to form iron nanoparticles at 750°C and finally, the carbonaceous material could cool obtaining carbon nanotubes [10].

2.4 Preparation of electrocatalysts

Electrocatalysts with a copper content of 10% w / w was prepared according to incipient impregnation method [11] using copper nitrate (Cu $(NO_3)_2$.5 H_2O (Auros Quimicos Ltda) as precursor. A certain amount of precursor is dissolved in 5 mL of water, after, 0.2 g of carbonuos materials are added. These samples were impregnated for approximately 20 minutes. Then it was subjected to heating at 50°C and 100°C for 12 hours respectively. Finally, the samples are subjected to nitrogen flow treatment at 350°C for 2 hours. The same procedure was used for the synthesis of other electrocatalysts using carbon nanotubes and activated carbon as support (Electrocat_carbonT, Electrocat_nanotubesC, Electrocat_GOR and Electrocat_EGOR).

The following nomenclature is used for identify the samples:

G: Commercial graphite.

EG: Electrochemical graphite.

GO: Commercial graphene oxide

EGO: Electrochemical graphene oxide

GOR: Reduced commercial graphene.

EGOR: Reduced electrochemical graphene

3. Results and Discussion

3.1 Materials: Figures 1-4 shown photos of synthesized materials (graphite oxidation and graphene reduction).

Figure 1. Commercial Graphene Oxide

Figure 2. Reduced commercial graphene.

Figure 3. Electrochemical graphene oxide.

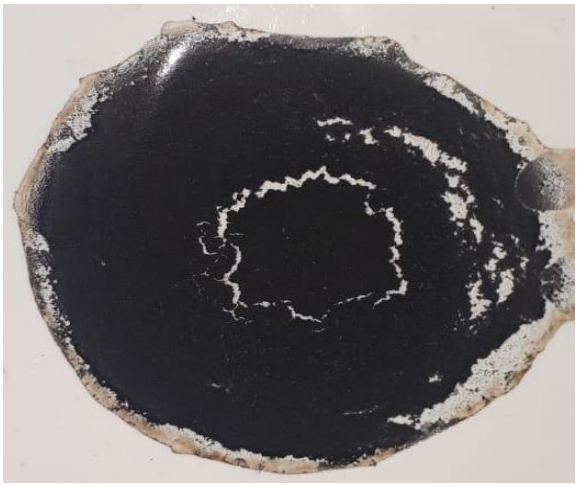

Figure 4. Reduced electrochemical graphene.

3.2 Raman spectroscopy

The Raman spectra of the samples are show in Figure 5 a and b. The Raman spectra displayed an intense band over 1600 cm^{-1} corresponding to fundamental vibrations within the aromatic layers of graphite, which is due to stretching of hybridized C-C carbon bonds [12-13]. The presence of this band is a fundamental characteristic of carbonaceous materials such as graphite [14]. In addition, an intense band is present at 1360 cm^{-1}, called so-called disorder-induced D-band. This band (D) is characteristic of poorly ordered materials and defective structures of graphite. Additionally, another weaker band can be observed in the 2650 cm^{-1} region, band called G' originate from a double resonance (DR) Raman process (second order band) [15].

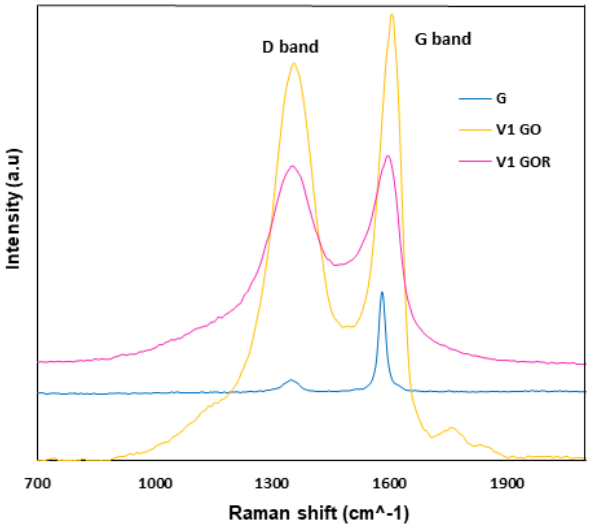

Figure 5a. The Raman spectrum of commercial graphite, graphene oxide, and reduced graphene oxide.

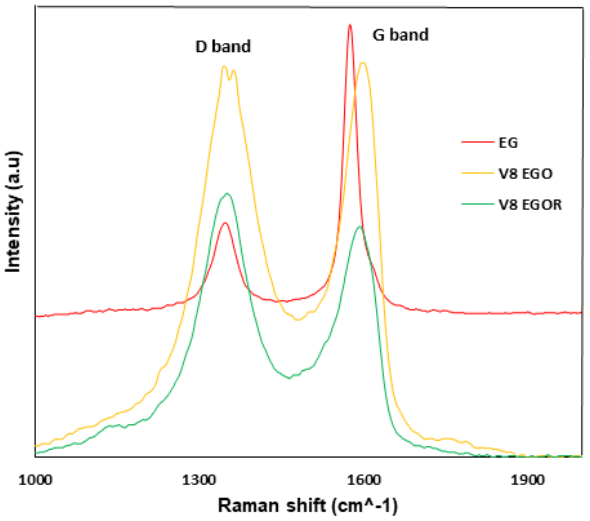

Figure 5b. The Raman spectrum of electrochemical graphite, graphene oxide, and reduced graphene oxide.

Figure 6 shows the reference patterns of graphene, indicating an intense band D of 1350 cm^{-1} approximately indicating the vibrations of the aromatic layers of graphite being characteristic of carbonaceous materials with defective structures of graphite and poorly ordered material. The presence of the intense band D' has been interpreted as an indicator of the high metamorphic face of chlorite, assigning to the carbonaceous material that presents this band [16]. In addition, another weaker band can be observed in the 2650 cm^{-1} region, the band called G' originates from a Raman double-resonance (DR) process (second order band) [16].

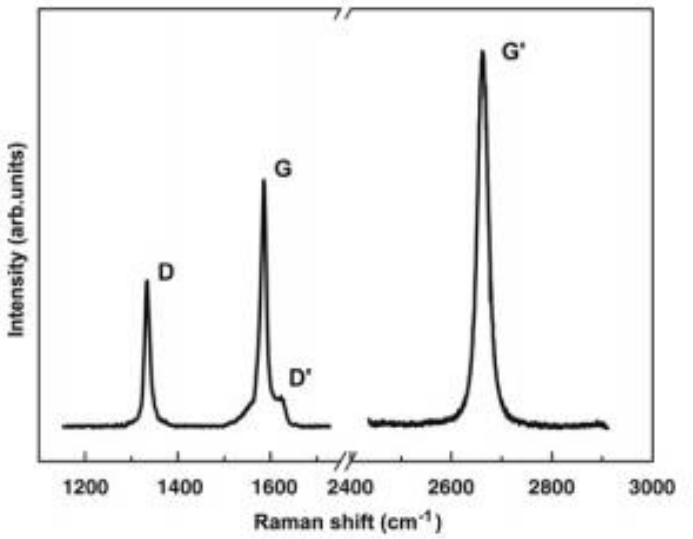

Figure 6. Raman spectrum of a graphene border, showing the main characteristics of Raman, the D, G and G 'bands taken with a laser excitation energy of 2.41 eV. [15].

All the samples (V6 GO, V8 EGO and V8 EGOR) prepared reflect the main bands and characteristics of graphene, such as bands D and D ', G and G', which confirm the nature of the synthesized material.

- **Normalized intensity:**

The spectra have been normalized to adjust the values to a common scale with a maximum value of 1 for the intensity, in Figures 7-8 the intensity that allows identifying each band is shown.

It is shown for the two synthesized materials (commercial and electrochemical graphite) present a D band at the position of 1350 cm^{-1} is intense and very broad, indicating a poorly ordered carbonaceous material, which depends preferentially of the wavelength of the incident laser [17]. During the graphitization process, the relative surface of the band D decreases with the arrangement of the aromatic planes. Consequently, this band has been attributed to defects such as heteroatoms (O, H and N) or structural defects [18]. The presence of this band is characteristic of graphene materials that have reached a degree of crystallinity. With the advance of metamorphism, the band becomes more acute and increases its intensity [19]. The G band, or graphite band, appears at the 1580 cm^{-1} position

and corresponds to the vibration mode of the crystal with symmetry [20] it is the characteristic band of natural graphite).

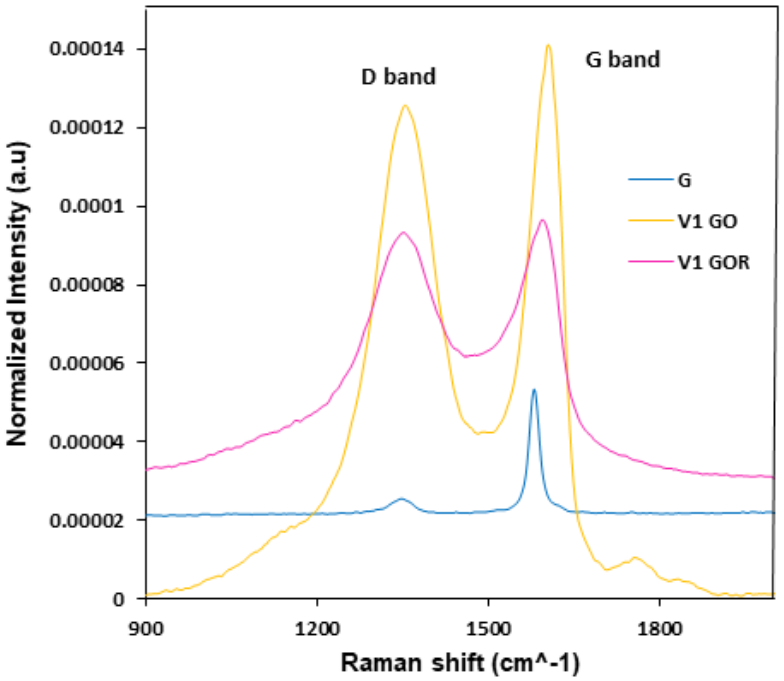

Figure 7. Normalized intensity of the Raman spectrum of commercial graphite, graphite oxide and reduced graphite.

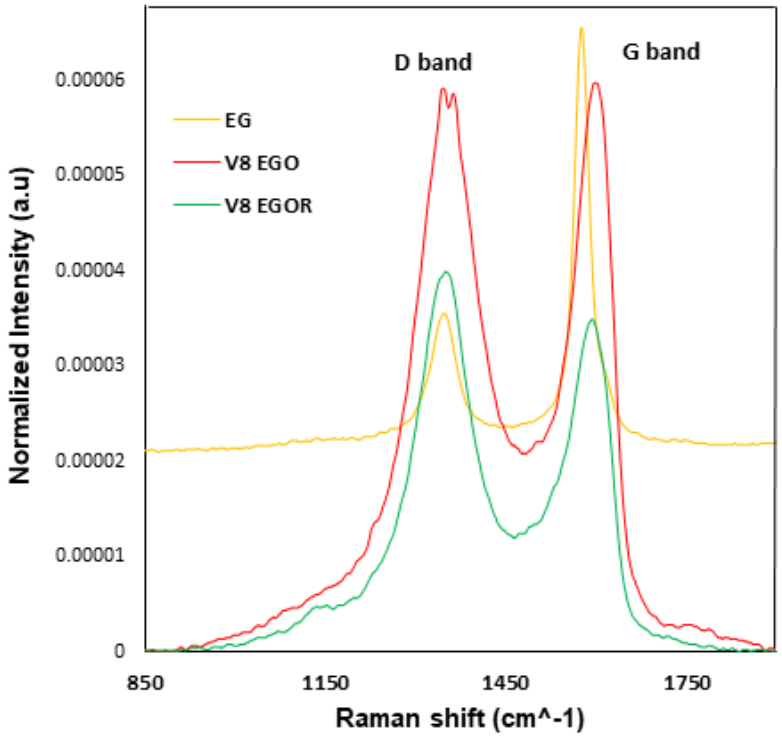

Figure 8. Normalized intensity of the Raman spectrum of electrochemical graphite, graphite oxide and reduced graphite.

Graphene oxides (V1 GO and V8 EGO) have D and G bands with different intensities, the D band indicates structural defects that show that the V1 GO sample has a greater number of defects with respect to V8 EGO, where the oxidation method of the Graphite affected its structure.

The sample V8 EGOR showed a lower intensity in the D and G bands compared to the V1 GOR samples indicating a lower defective distribution of the characteristic graphitic structure of the materials with low crystallinity, this comparison can be observed with the Raman spectrum of the graphite without synthesize.

- **Reproducibility of graphene prepared.**

In order to study the reproducibility of graphene, different samples have been synthesized (V1 GO and V6 GO). Figure 9 shows that they are reproducible, since the two samples have the same intense band D at 1350 cm^{-1} and intense band G in 1600 cm^{-1}. Since this sample represents the typical carbonaceous material with a greater structural order, concluding that the samples synthesized in the laboratory are reproducible.

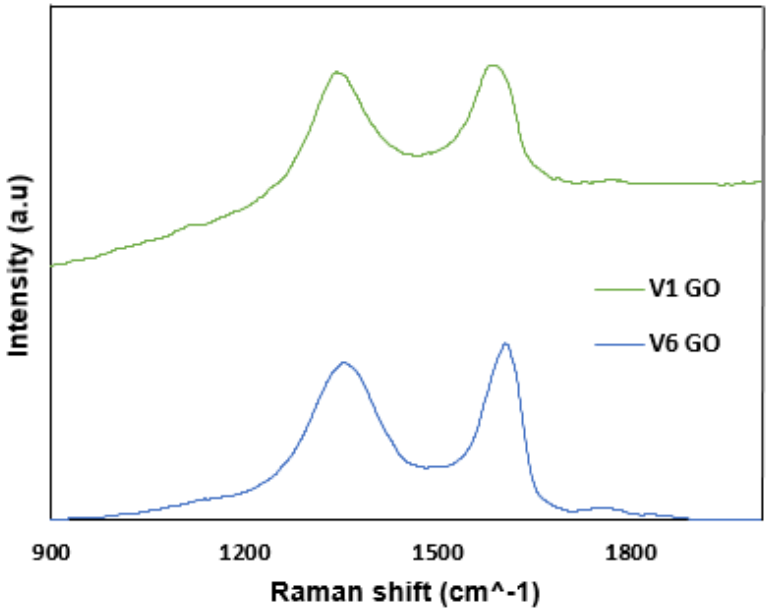

Figure 9. Reproducibility of commercial graphene oxide.

According to Figure 10 the samples V3 EGO and V8 EGO are reproducible due to their bands appear at the same wavelength in their Raman spectral. There are some minimal differences, the V3 EGO sample has a better structural order, while the V8EGO sample have the D band has greater, which is related to the structural degree disorder, because they have an origin related to a loss of symmetry due to the finite size of the graphite crystals, or due to the stretching vibration in the sp2 and sp3 hybridized bonds of the carbon atoms [21].

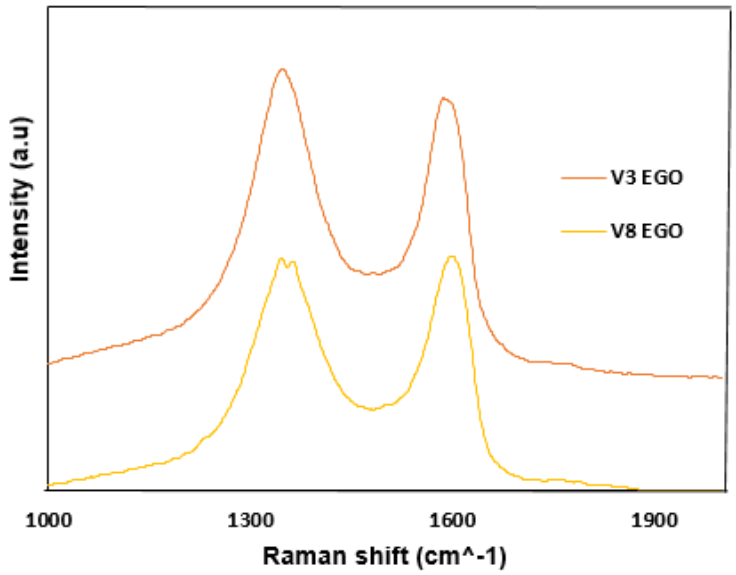

Figure 10. Reproducibility of electrochemical graphene oxide.

Respect to V3EGOR and V8EGOR samples, these coincide in the same wavelength for both D and G bands (see, Figure 11). Finally, it is possible to conclude that preparation method for produce reduced graphed is satisfactory [22].

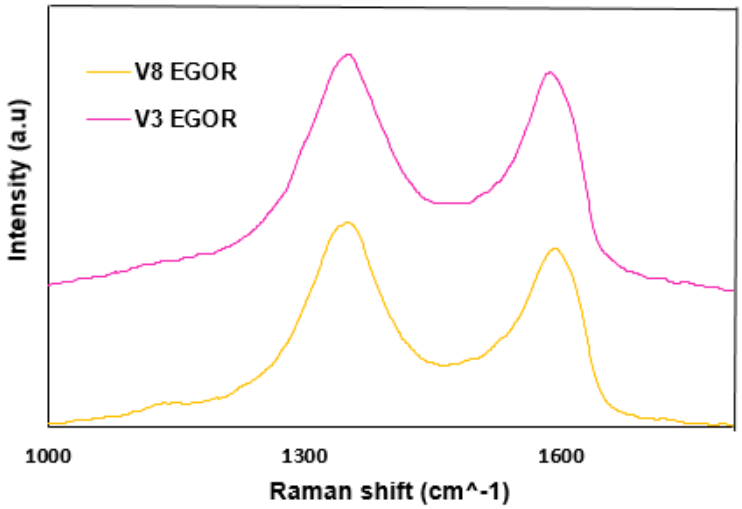

Figure 11. Reproducibility of Reduced electrochemical graphene.

3.3 XRD Characterization

Figures 12 and 13 show the XDR patterns of graphene synthesized. Initially, Figure 12 shows the characteristic band that can be observed (at 26.6 °) of both carbonaceous materials for commercial and electrochemical graphite used as a raw material [23]. In addition, the peak present in, from 12 ° to 25 °, indicates that the graphite is incompletely oxidized [24].

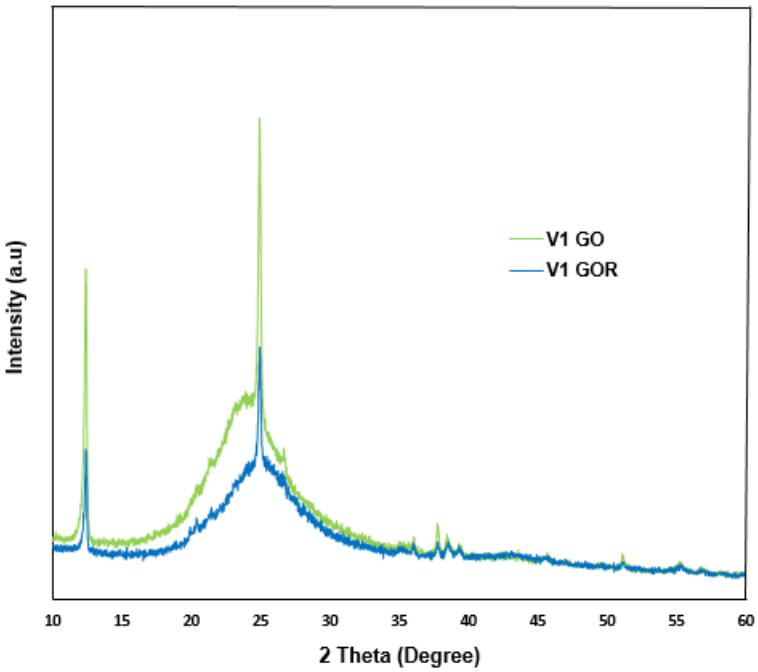

Figure 12. X-ray diffraction (XRD) of graphene oxides and graphene reduced by commercial graphite.

According to Figure 13, it shows the shape of the line for the samples (V3 EGO and V3 EGOR) tends to be similar, but in some cases it has a marked asymmetric line, which is representative of the different curves, this is due to the different batch used in the synthesis and origin of different graphite [25].

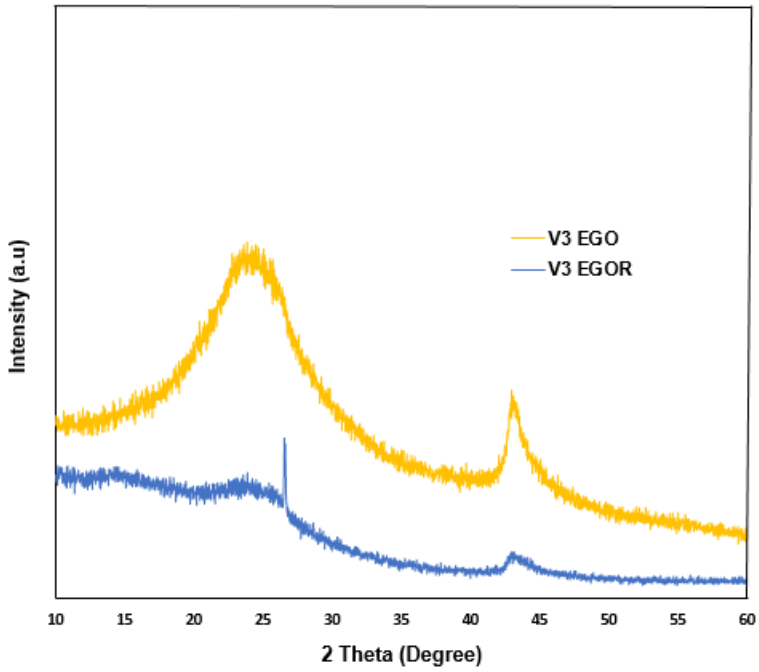

Figure 13. X-ray diffraction (XRD) of graphene oxides and graphene reduced by electrochemical graphite.

It can observed that samples prepared show different values of FWHM (Full Width at Half Maximum), These values are important because they show how susceptible the material; that is, the lower the value, the lower are the defects and impurities in the sample, although for these samples they show higher value, likewise, they move at greater angles with respect to the reference of the angular position of the graphite [26].

Table 1 shows the values of FWHM of the diffraction curves, indicating the crystal quality of each sample of synthesized graphene.

Table 1. Width at half height (FWHM) of the main peaks of the graphite samples.

Sample	FWHM (degrees)
V3 EGOR	38,03118 ± 0,66372
V3 EGO	7,86974 ± 0,06928
V1 GOR	0,2797 ± 0,01403
V1 GO	0,26985 ± 0,00921

With the previous values presented in Table 1, it is concluded that for commercial and electrochemical samples of graphite there is a lower distribution of defects for both commercial and electrochemical samples, with relatively lower values of FWHM of 0.19147 ± 6.90598E-4 and 0.48108 ± 0.0026 respectively in comparison with the samples synthesized in the laboratory.

In relation to the above, it can be announced that the purification process applied to samples V1 GO and V1 GOR caused significant damage to the graphite structure by eliminating carbon, amorphous and metal nanoparticles.

Regarding the average value for the sample V3 EGOR is higher than all the samples worked, presenting a value for FWHM = 38.03118 ± 0.66372 indicating that the reduction process affected its structure. While the sample V3 EGO presents a value for FWHM: 7.86974 ± 0.06928 indicating the characteristics of the sample.

3.4 Infrared spectroscopy

Figure 14 shows the FTIR spectra obtained from the commercially synthesized graphite and its respective graphene oxide, showing the presence of chemical functionalities such as OH (3691 cm-1), OH (2344 cm-1), C_ = C (2113 cm -1) terminal alkyne, C = O (1700 cm-1), C = C (1645cm-1), CO of the epoxy groups 1228 cm-1 and CO vibrations of the alkoxide groups 1059 cm-1 [27]. Figure 15 shows the electrochemical graphite and its respective graphene oxide, presenting its functional groups such as OH (2344 cm-1), C_ = C (2113 cm-1) terminal alkyne, C = O (1701 cm-1) and C = aromatic C (1568 cm-1) with a strong to weak bond in their interactions. Additionally, the V8 EGO sample has a wide band of 2116 cm-1 accompanied by the narrow, well-defined peak that corresponds to the stretching vibration of the carbonyl group [27].

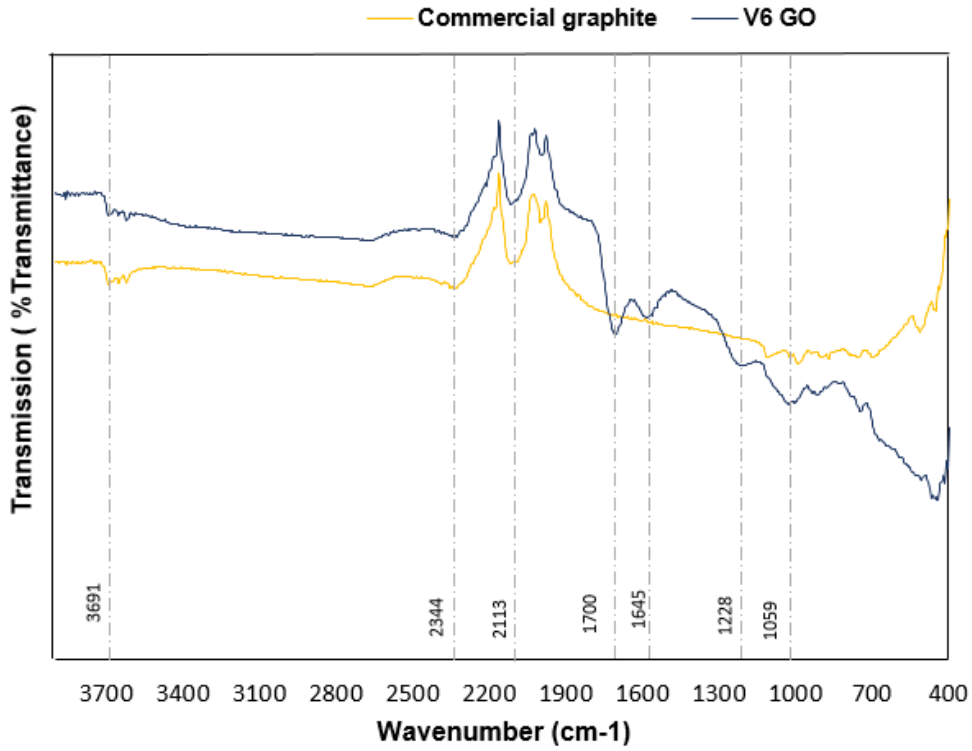

Figure 14. Infrared spectroscopy of electrochemical graphite and commercial graphene oxide

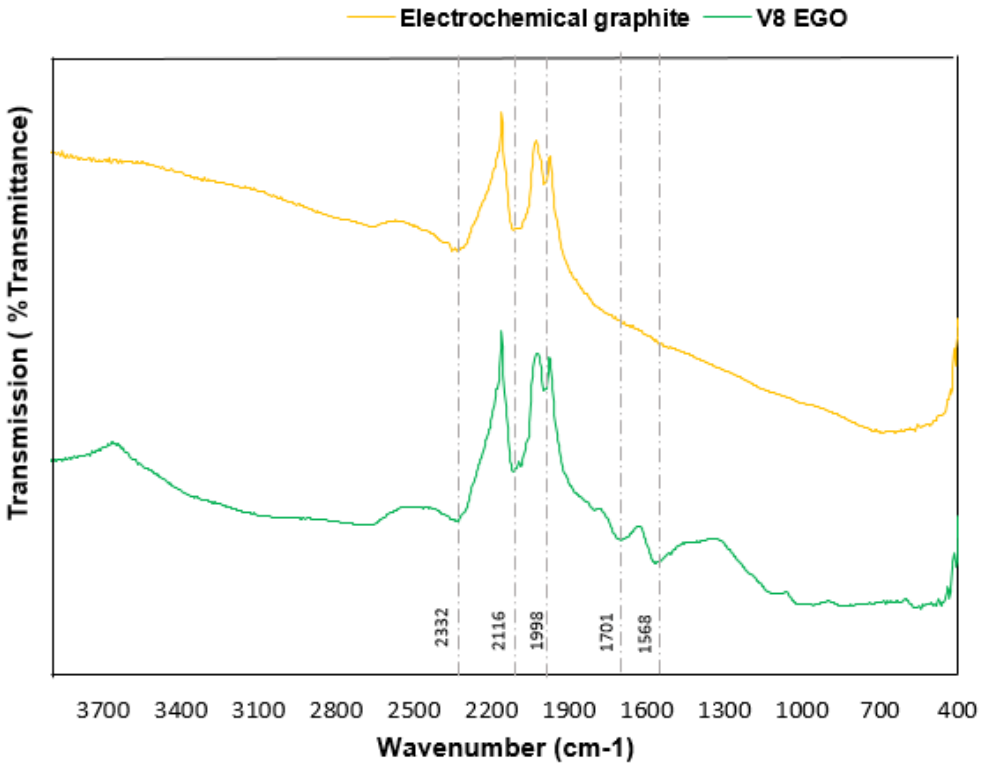

Figure 15. Infrared spectroscopy of electrochemical graphite and electrochemical graphene oxide

Therefore, the samples V8 EGO and V6 GO, show greater definition in the bands of the spectrum. By analyzing both spectra, it is possible to contemplate the characteristics of the reference spectra of oxidized graphene in which the same bands can be observed, since the signals associated with the vibrations C = O and C = C have given rise to a single band at 1645 cm -1 related to the stretching vibration C = O.

Finalizing with the FTIR spectrum of the catalysts produced with different supports, it was analyzed according to Figure 16 that all the samples presented the same bands, that is to say the same functional groups, such as OH (2339 cm -1), C = terminal C-alkyne (2111 cm-1) with weak stretching and between other functional groups that were not evidenced by the spectrum, perhaps due to the minimal amount present in the sample [28].

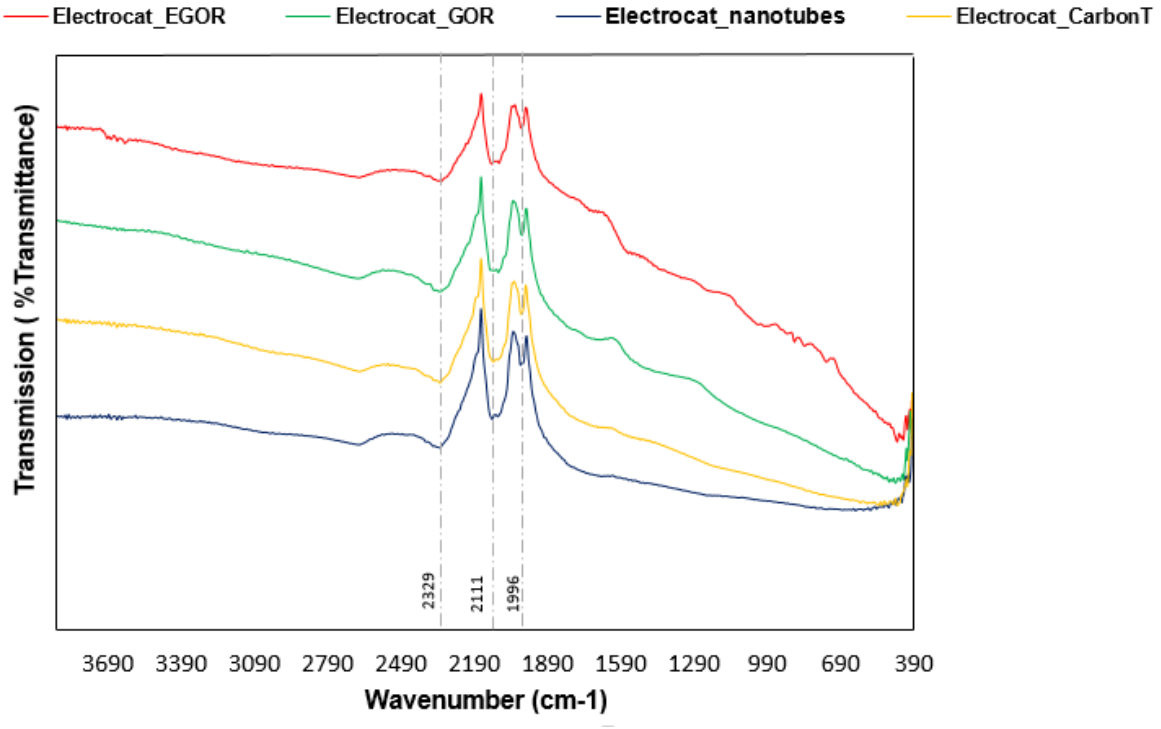

Figure 16. Infrared spectroscopy of electrocatalysts.

SEM Characterization

Figures 17 and 18 show the microphotos of V6 GO and V8 EGO samples, graphene sheets having smooth surfaces. The samples were in an oxidation process allowing the formation of intercalation compounds between the sheets of graphene, where there was a functionalization of the edge in the oxidation of the graphite and in the exfoliation through the process of synthesis of the material [29].

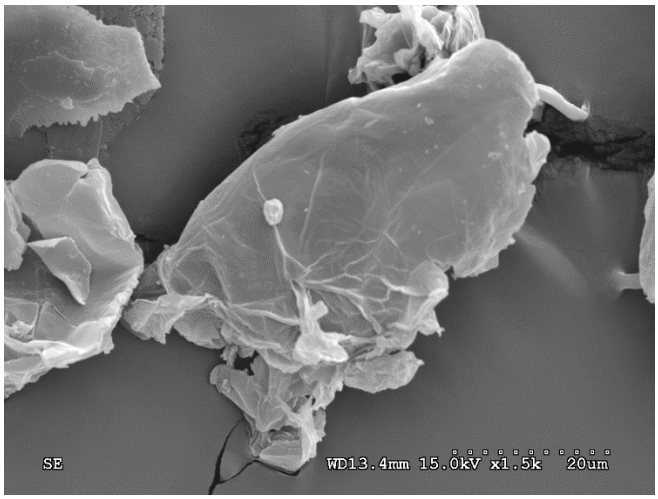

Figure 17. V6 GO (commercial graphene oxide) with an increase of 20 um.

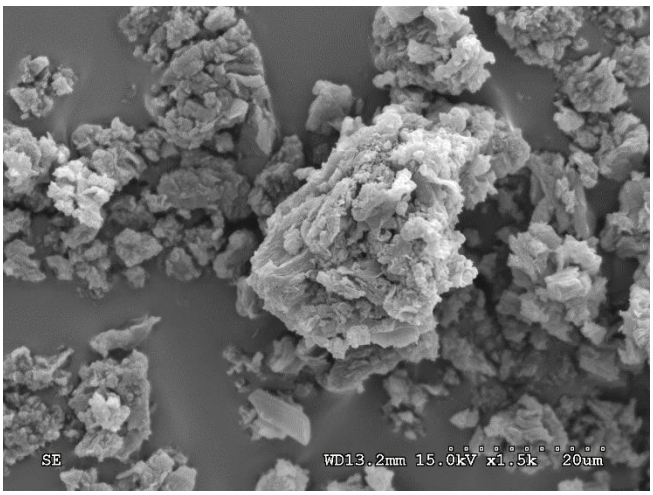

Figure 18. V8 EGO (Electrochemical graphene oxide) with an increase of 20 um.

Figures 19-20 shown electrocatalysts produced with 10% Cu supported on electrochemical graphene and supported on commercial graphene, respectively, showing the grain size generated by the copper coating, since it reduces the roughness of the surface, without presenting a typical morphological surface of the ridges and valleys. However, the sample of GOR 10 Cu will be the one that provides the least copper coating due to its particle size, since it is smaller in comparison with the other support (electrochemical graphene). On the contrary, the sample EGOR 10 Cu presented small copper particles, differentiating the fibers from the carbonaceous support of the added metal [29]. As observed in both samples, the metal deposits are crystalline in both cases [29].

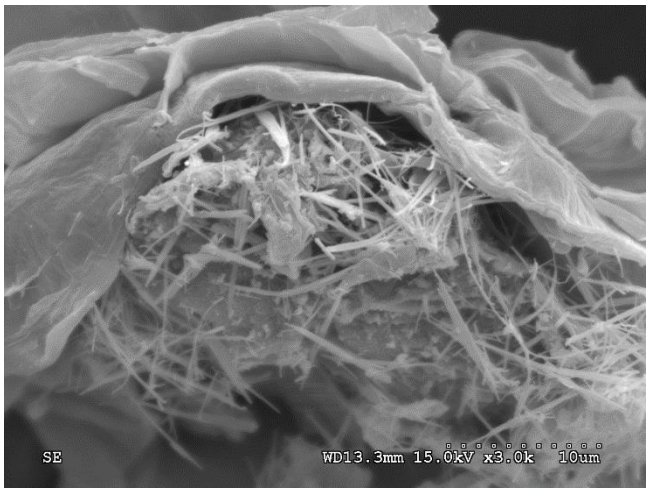

Figure 19. EGOR 10 Cu (10% copper electrocatalyst (m / v) supported on electrochemical graphene)

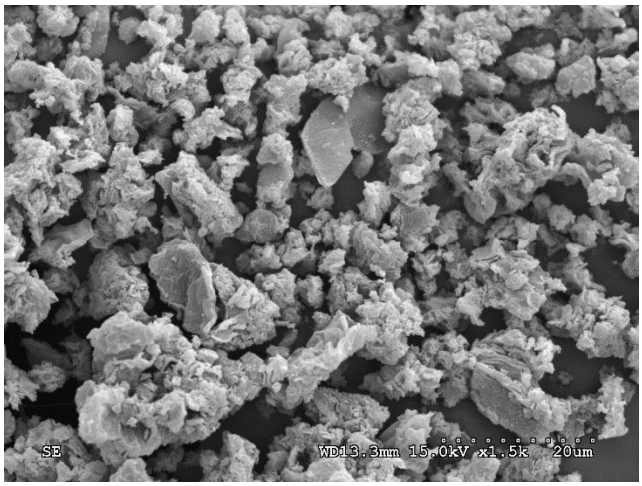

Figure 20. GOR 10 Cu (10% copper electrocatalyst (m / v) supported on commercial graphene)

The sample V6 GO and V8 EGO presented a very different morphology to the samples EGOR 10 Cu and GOR 10 Cu, since it has a high content of oxygen, so these samples must be highly functionalized, changing significantly. This effect may be related to the change in carbon hybridization, promoted by the oxidation reaction. In conclusion, with a longer oxidation time, structures with higher content of intercalation compounds are obtained in the graphene layers [29].

Conclusions

In this research, the characterizations made by Raman and XRD spectroscopy confirm that both the commercial graphene oxide and the electrochemical, synthesized by the modified Hummer method, present intense bands above 1600 cm^{-1} characteristics of carbonaceous materials such as graphite that has reached a degree of crystallinity. In addition, they presented an intense contiguous band in the 1360 cm^{-1} zone called band D, which indicates

the defective structures and the poorly ordered material of the graphite, indicating that the modified Hummer method has good experimental acceptability.

Adding to the above, the most important results obtained by the SEM characterization to copper electrocatalysts supported on graphene of commercial origin confirmed that they are efficient for the carbon dioxide reduction reaction, since it presents a better copper coating compared to other materials, improving their specific properties. And at the same time its performance in electroreduction.

Acknowledgment

The authors thank the funds provided to the project "Electrocatalytic revaluation of CO_2 using copper and iron catalysts supported in graphene" funded by the University Development Cooperation Unit and the University of Bogotá Jorge Tadeo Lozano.

References

[1] D. S. Simakov, «Fundamentals, Catalysis, Design Considerations and Technological Challenges,» de *Renewable Synthetic Fuels and Chemicals from Carbon Dioxide*, Springer International Publishing, pp. VIII, 69.

[2] «Carbon-based electrocatalysts for advanced energy conversion and storage,» *ScienceAdvances,* vol. 1, nº 7, 2015.

[3] N. Gutierrez Guerra, L. Moreno López, J. C. Serrano Ruiz, J. L. Valverde y A. De Lucas Consuegra, «Gas phase electrocatalytic conversion of CO2 to syn-fuels on Cu based catalysts-electrodes,» *ScienceDirect,* vol. 188, pp. 272-828, 2016.

[4] Y. Hori, I. Takahashi, O. Koga y N. Hoshi, «Electrochemical reduction of carbon dioxide at various series of copper single crystal electrodes,» *ScienceDirect ,* vol. 199, nº 1-2, pp. 39-47, 2003.

[5] W. Tang, A. A. Peterson, A. S. Varela, Z. P. Jovanov, L. Bech, W. J. Durand, S. Dahl, J. K. Norskov y L. Chorkendorff, «The importance of surface morphology in controlling the selectivity of polycrystalline copper for CO2 electroreduction.,» *Royal Society of Chemistry,* vol. 14, pp. 76-81, 2012.

[6] S. Park y R. S. Ruoff, «Chemical methods for the production of graphenes.,» *US National Library of Medicine National Institutes of Health,* pp. 217-24, 2009.

[7] H. Qinggang, L. Quing , K. Samson, R. Xiaoming, F. E. López Suarez, D. Lozano Castelló, A. Bueno López y G. Wu, «High-Loading Cobalt Oxide Coupled with Nitrogen-Doped Graphene for Oxygen Reduction in Anion-Exchange-Membrane Alkaline Fuel Cells,» *The Journal of physical chemistry,* p. 117, 2013.

[8] P. Sampedro Tejedor, A. Maroto Valiente, D. M. Nevskaia, I. Rodriguez, I. Rodriguez Ramos y A. Guerrero Ruiz, «The effect of growth temperature and iron precursor on the synthesis of high purity carbon nanotubes,» *ELSEVIER,* vol. 16, nº 3, pp. 542-549, 2007.

[9] M. Perez Cardenas, A. Muñoz , I. Rodriguez Ramos, A. Maroto Valiente y A. Guerrero Ruiz, «Building up multiwall carbon nanotubes nanostructures inside,» *Journal of Nano Research,* Vols. %1 de %218-19, pp. 271-279, 2012.

[10] F. E. López Suarez, A. Bueno López, M. J. Illán Gomez, B. Ura y J. Trawczynski, «Study of the uncatalyzed and catalyzed combustion of diesel and biodiesel soot,» *ScienceDirect,* vol. 176, nº 1, pp. 182-186, 2011.

[11] M. R. Ammar y J. N. Rouzaud, «How to obtain a reliable structural characterization of polished graphitized carbons by Raman microspectroscopy,» *Journal of Raman Spectoscopy,* vol. 43, nº 2, 2011.

[12] T. Kim, C. Jo, W. G. Lim, J. Lee, L. Jaegeun y K.-H. Lee, «Facile conversion of activated carbon to battery anode material using microwave graphitization,» *ScienceDirect,* vol. 104, pp. 106-111, 2016.

[13] P. K. Chu y L. Li, «Characterization of amorphous and nanocrystalline carbon films,» *ScienceDirect,* vol. 96, nº 2-3, pp. 253-277, 2006.

[14] R. Navratil, A. Kotzianova, V. Halouzka, T. Opletal, I. Triskova, L. Trnkova y J. Hrbac, «Polymer lead pencil graphite as electrode material: voltammetric, XPS and Raman study,» *ScienceDirect,* vol. 783, pp. 152-160, 2016.

[15] K. Ushizawa, K. Watanabe, T. Ando, I. Sakaguchi, M. Nishitani-Gamo, Y. Sato y H. Kanda, «Boron concentration dependence of Raman spectra on {100} and {111} facets of B-doped CVD diamond,» *ELSEVIER,* vol. 7, nº 11-12, pp. 1719-1722, 1998.

[16] O. Beyssac, B. Goffe, C. Chopin y J. N. Rouzaud, «Raman spectra of carbonaceous material in metasediments: a new geothermometer,» *Journal of Metamorphic Geology,* vol. 20, nº 9, 2002.

[17] J. N. Rouzaud, A. Oberlin y C. Beny-Bassez, «Carbon films: Structure and microtexture (optical and electron microscopy, Raman spectroscopy),» *ELSEVIER,* vol. 105, nº 1, pp. 75-96, 1983.

[18] S. Reich y C. Thomsen, «Raman spectroscopy of graphite,» *The Royal Society,* 2004.

[19] P. K. Rohatgi, Y. Liu, M. Yin y T. L. Barr, «Materials Science and Engineering A,» vol. 123, pp. 213-218, 1990.

[20] K. Naplocha y K. Granat, «Achieves of Materials Science and Engineering,» *ScienceDirect,* vol. 29, nº 2, pp. 81-88, 2008.

[21] P. Szirmai, T. Pichler, O. A. Williams, S. Mandal, C. Bauerle y F. Simon, «A detailed analysis of the Raman spectra in superconducting boron doped nanocrystalline diamond,» *ELSEVIER,* vol. 249, nº 12, 2012.

[22] S. A. El-Khodary, G. M. El-Enany, M. El-Okr y M. Ibrahim, «Preparation and characterization of microwave reduced graphite oxide for high performance supercapacitors,» *ScienceDirect,* vol. 150, pp. 269-278, 2014.

[23] G. Rantitsch, W. Lammerer, E. Fisslthaler, S. Mitsche y H. Kaltenbock, «Heidi, On the discrimination of semigraphite and graphite by Raman spectroscopy,» *ScienceDirect,* vol. 159, pp. 48-56, 2016.

[24] «Raman spectroscopy of graphene and graphite: Disorder, electron–phonon coupling, doping and nonadiabatic effects,» *ELSEVIER,* vol. 143, nº 1-2, pp. 47-57, 2007.

[25] K. Taewon, J. Changshin, L. Won-Gwang, L. Jaegeun , L. Jinwoo y L. Kun-Hong, «Facile conversion of activated carbon to battery anode material using microwave graphitization,» *ScienceDirect,* vol. 104, pp. 106-111, 2016.

[26] A. Oberlin y M. Oberlin, «Graphitizability of carbonaceous materials as studies by TEM and X-ray diffraction,» *Journal of Microscopy,* vol. 132, nº 3, 1983.

[27] L. Martin Ortin, «Escuela Ténica Superior de Ingenieros,» [En línea]. Available: http://bibing.us.es/proyectos/abreproy/20406/fichero/PFC_Lara+Mart%C3%ADn+Ortin.pdf. [Último acceso: 1 Septiembre 2018].

[28] Campos Tapia, V. (Octubre de 2013). *UNIVERSIDAD AUTÓNOMA DE NUEVO LEÓN.* Obtenido de PREPARACIÓN Y CARACTERIZACIÓN DE GRAFENO MODIFICADO CON NANOPARTICULAS METÁLICAS Y BIMETÁLICAS: http://eprints.uanl.mx/3282/1/1080256740.pdf

[29] Yapu , E. L., Blanco, M., Cabrera, S., Balanza, R., & Yapu, W. (2013). OXIDO DE GRAFITO EXTENDIDO. *Revista Boliviana de Química*, 156-161.